

# The physical interpretation of the parameters measured during the tensile testing of materials at elevated temperatures

B. BURTON

*Central Electricity Generating Board, Berkeley Nuclear Laboratories, Berkeley, Gloucestershire, UK*

Hot tensile (or compression) testing, where the stress developed in a material is measured under an imposed strain rate, is often used as an alternative to conventional creep testing. The advantages of the hot tensile test are that its duration can be more closely controlled by the experimenter and also that the technique is more convenient, since high precision testing machines are available. These factors can be particularly important when extensive testing programmes of radioactive samples are involved. The main disadvantage is that the interpretation of results is more complex. Confusion can easily arise when attempts are made to extend the use of parameters which satisfactorily categorize behaviour at lower temperatures, into regimes where concurrent thermal recovery can occur. The present paper relates the parameters which are measured in hot tensile tests, to physical processes which occur in materials deforming by a variety of mechanisms. For cases where no significant structural changes occur, as in viscous or superplastic flow, analytical expressions are derived which relate the stresses measured in these tests to material constants. When deformation is controlled by recovery processes, account has to be taken of the structural changes which occur concurrently. A wide variety of behaviour may then be exhibited which depends on the initial dislocation density, the presence of second-phase particles and the relative values of the recovery rate parameters and the velocity imposed by the testing machine. Numerical examples are provided for simple recovery models.

## 1. Introduction

The mechanical properties of materials at elevated temperatures are usually measured either by using creep tests, where the time dependence of strain is recorded for a certain applied stress, or by measuring the stress which is developed in the material under some imposed strain rate. The interpretation of results from the first type of test is reasonably straightforward, particularly when it can be arranged for the stress to be maintained at a constant level during the test. The latter type of test, often called the hot tensile test (or compression test) is somewhat more difficult to interpret, although is often convenient to perform mainly because of the availability of precision testing

machines. Such machines have been developed for more conventional tests at lower temperatures when no concurrent thermal recovery is occurring. If a means exists of interpreting high temperature data from the same equipment, then this provides a more convenient means of obtaining fundamental information. This can be particularly important for radioactive samples which require extensive shielded facilities.

The basic differences between the two modes of testing may be categorized in terms of the rates of energy dissipation and the availability of a deformation mechanism. In a creep test, the material simply deforms by the mechanism which occurs at the fastest rate at the particular stress

level of test. Thus, in cases where structural changes occur, the strain rate also changes with time accordingly. In the hot tensile test, such strain rate changes are not possible since the specimen is forced to deform at a rate dictated by the crosshead velocity. As a consequence, the stress developed in the specimen must change in order for the deformation rate to match this velocity.

During steady state deformation, it is clear that the measured rate and the applied stress in the creep test are equivalent to the imposed deformation rate and the measured steady state flow stress in the hot tensile test. It should be noted that in a "cold" tensile test, no steady state flow stress is obtained, since work hardening continues up to the point of failure at the ultimate tensile strength (UTS). In the hot test, the steady state flow stress for a recovery creep mechanism is that level of stress where the rate of hardening due to the imposed strain rate is just balanced by the rate of thermal softening. The apparent similarity between the shapes of the curves from hot and cold tests and the gradual nature of the change in the type of behaviour between the two, has often led to considerable confusion in the interpretation of the stresses measured from this type of test.

The aim of the present paper is to analyse the stress-time behaviour for hot tensile tests and to indicate the relationships between creep behaviour, the apparent UTS and the proof stress (PS). (The PS is a commonly used parameter in tensile tests. It is taken to be the flow stress at some conveniently defined level of strain. Its value may be substantially less than the steady state flow stress for small reference strains or equal to it, if the strain is sufficiently high.) It should perhaps be emphasized that because of the convenient and often more rapid nature of the hot tensile test, it is commonly used in the manner of a "quality control" test. Under such conditions, the concept of a high temperature PS and UTS may be an entirely satisfactory means of providing reference data. This paper is concerned with the relationship between these parameters and fundamental properties of the material. Of current interest at Berkeley Nuclear Laboratories is the possibility of estimating the creep parameters of irradiated PE16 tie-bar material from in-cell tensile tests at reactor discharge temperatures. These fundamental parameters are required for present

physical model-based safety codes concerning fuel discharge.

## 2. Stress-time behaviour

A material will be considered which obeys a creep equation of the form:

$$\dot{\epsilon} = \alpha(\sigma - \sigma_0)^n \quad (1)$$

where  $\dot{\epsilon}$  is the tensile creep rate under constant tensile stress  $\sigma$ ,  $\alpha$  is a constant which contains thermodynamic, structural and material parameters,  $n (\geq 1)$  is the stress index and  $\sigma_0 \geq 0$  is a threshold value of stress below which  $\dot{\epsilon} = 0$ . For materials which deform by a mechanism which involves no structural changes, the creep rate does not depend on previous history, it depends only on stress. As a simple illustration, the viscous flow rate of a simple fluid depends only on the instantaneous value of pressure gradient and, for crystalline solids, diffusional creep corresponds to an equivalent case. The structural feature which dictates the creep rate is the grain size, so that if this remains constant, the instantaneous value of stress is sufficient to describe the rate. Superplastic deformation provides a similar example. The salient structural feature is again the grain size so once again, if this stays constant, the instantaneous value of stress dictates the rate.

In recovery creep, where strain hardening and thermal recovery act in conjunction, an equation of the type shown above is often used to describe the steady state creep rate. The equation only has relevance when the two processes, hardening and recovery, operate at matching rates. As a consequence, serious errors are possible if predictions of behaviour during stress transients are attempted, using empirical equations obtained under steady state conditions. It is important to bear in mind this distinction between these two types of flow behaviour. Both can be represented by the relationship of Equation 1, but a fundamental difference lies in the interpretation of behaviour during stress transients.

### 2.1. Newtonian viscous behaviour

The testing apparatus will be assumed to be a constant velocity device which drives an elastic connection to the specimen. This elastic connection usually consists of the beam of the testing machine and the pull-rods.

It is clear that the rate at which the stress builds up in the specimen ( $d\sigma/dt$ ) is equal to the

difference between the rate of increase of elastic stress due to the deflection and the rate of decay due to plastic creep. The governing differential equation is:

$$\begin{aligned} \frac{d\sigma}{dt} &= \left\{ \frac{1}{K+l/E} \right\} \frac{dx}{dt} - \left\{ \frac{l}{K+l/E} \right\} \frac{d\epsilon}{dt} \\ &= \left\{ \frac{1}{K+l/E} \right\} \{V - l\dot{\epsilon}\} \end{aligned} \quad (2)$$

where  $K$  is the elastic constant of the connection, defined here as the deflection per unit stress on the specimen,  $l$  is the gauge length,  $E$  the elastic constant of the material and  $V (= dx/dt)$  the cross-head velocity. The equation is now solved for the case of a Newtonian solid.

In a Newtonian solid, the creep rate varies linearly with applied stress ( $\sigma_0 = 0$  and  $n = 1$  in Equation 1). For crystalline solids this may correspond to diffusional creep [1] with no accompanying grain growth or other transient component. The creep constant is then  $\alpha = \alpha_1 = 10 \Omega D/d^2 kT$  for lattice diffusion control, where  $D$  is the diffusion coefficient,  $\Omega$  the atomic volume,  $d$  the grain size,  $k$  is Boltmann's constant the  $T$  the temperature in Kelvin. For grain-boundary diffusion control  $\alpha = \alpha_2 = 50 \Omega \omega D_g/d^3 kT$ , where  $\omega$  is the boundary width and  $D_g$  the boundary diffusion coefficient. Substitution of  $\dot{\epsilon} = \alpha \sigma$  into Equation 2 and integrating with the conditions that  $\epsilon = 0$  at  $t = 0$  gives the variation of stress with time to be:

$$\sigma = \frac{V}{\alpha l} \left[ 1 - \exp \left( - \frac{\alpha l t}{K + l/E} \right) \right]. \quad (3)$$

At short times, the expansion  $\exp x \sim 1 + x$  may be used to give the initial form of the  $\sigma, t$  curve. That is  $\sigma = Vt/(K + l/E)$ , so that a linear elastic variation of stress with time will be observed. The curve decays exponentially to the steady state flow stress at long times. This is, when  $\sigma = V/\alpha l$ . Clearly the creep constant can be obtained directly from this relationship.

Often, the proof stress provides a more convenient parameter to determine experimentally. The relationship between PS and the steady state flow stress (or apparent UTS – denoted "UTS") can be obtained by considering the form of the plastic strain–time relationship. From Equations 1 and 3:

$$\frac{d\epsilon}{dt} = \alpha \sigma = \frac{V}{l} \left( 1 - \exp - \frac{\alpha l t}{K + l/E} \right). \quad (4)$$

Integration of this equation, again noting that

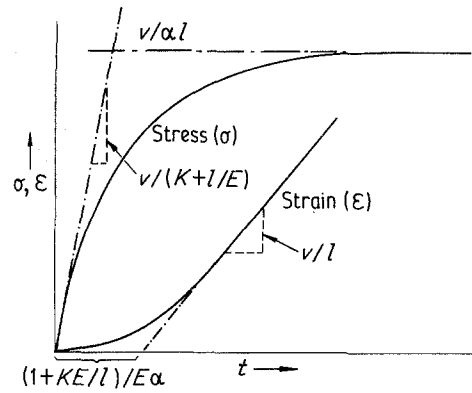


Figure 1 Variation of stress and strain with time for a Newtonian viscous material tested at constant crosshead velocity. Parameters are defined in the text.

$\epsilon = 0$  at  $t = 0$  gives the strain–time relationship as follows:

$$\epsilon = \frac{V}{l} \left[ t - \frac{K + l/E}{\alpha l} \left( 1 - \exp - \frac{\alpha l t}{K + l/E} \right) \right]. \quad (5)$$

Note that at long times:

$$\epsilon = \frac{V}{l} \left( t - \frac{K + l/E}{\alpha l} \right) \quad (6)$$

and in the case of a stiff machine where  $K = 0$ , then:

$$\epsilon = \frac{V}{l} \left( t - \frac{1}{\alpha E} \right). \quad (7)$$

The relationships between the various parameters are shown in schematic form in Fig. 1.

In order to determine an analytical relationship for the proof stress, it is required to obtain the time at which a certain strain is reached and then substitute for  $\sigma$  in Equation 3. To a sufficient level of accuracy, the exponential term in Equation 5 can be expanded in the form  $\exp x = 1 + x + x^2/2$  which gives the time to reach a strain  $\epsilon^*$  as

$$t^* \sim \left[ \frac{2(K + l/E)}{\alpha V} \epsilon^* \right]^{1/2} \quad (8)$$

and substituting for  $t^*$  in Equation 3 gives the proof stress:

$$\sigma_{PS} = \frac{V}{\alpha l} \left[ 1 - \exp - \left( \frac{2\alpha l^2 \epsilon^*}{V(K + l/E)} \right)^{1/2} \right] \quad (9)$$

Since  $V/\alpha l$  is the steady state flow stress, this equation gives the PS/"UTS" ratio directly.

## 2.2. Nonlinear creep behaviour for constant structure

### 2.2.1. Superplastic behaviour

Under conditions of ultra-fine grain size and at intermediate stress levels, materials often creep in such a way that the rate is proportional to the square of the stress. Such behaviour is termed superplastic. The main structural feature which dictates the mechanical response is the grain size. If this is constant during test then an analysis can be performed similar to that in the previous section. Substitution of  $\dot{\epsilon} = \alpha \sigma^2$  into Equation 2 followed by integration, gives the stress–time dependence.

$$\sigma = \left( \frac{V}{\alpha l} \right)^{1/2} \tanh \left[ \frac{Vt}{K + l/E} \left( \frac{\alpha l}{V} \right)^{1/2} \right] \quad (10)$$

where  $(V/\alpha l)^{1/2} \equiv$  “UTS” and  $\alpha = \alpha_3$  is the creep constant for superplastic flow. The strain–time dependence is given by:

$$\epsilon = \frac{Vt}{l} - \frac{K + l/E}{l} \left( \frac{V}{\alpha l} \right)^{1/2} \tanh \left[ \frac{Vt}{K + l/E} \left( \frac{\alpha l}{V} \right)^{1/2} \right] \quad (11)$$

### 2.2.2. Power law creep

Diffusional creep and superplastic deformation can, in principle, proceed with no requirement for significant structural changes. The processes depend on diffusional fluxes between grain boundaries and on boundary sliding, so that in the absence of grain coarsening, the requirements of the previous analyses can be met. For dislocation recovery creep, however, it is the mean dislocation spacing which characterizes the rate of deformation. Thus, unlike the previous cases where the characteristic dimension (the grain size) remains unchanged, the dislocation density can now vary in response to the applied stress (or strain rate). As a consequence, the condition of constant structure during test is no longer valid. Nevertheless it is instructive to construct hypothetical curves assuming that the power law equation for recovery creep is valid at any instantaneous value of stress during a transient. Such an assumption requires that the structure changes instantaneously to that appropriate to the instantaneous value of stress. This is clearly not the case during recovery creep since a finite time is required for structural changes to occur. The exercise is useful, however, in that it enables comparisons with the cases considered later where structural changes are allowed to occur in finite times. This permits estimates to be made

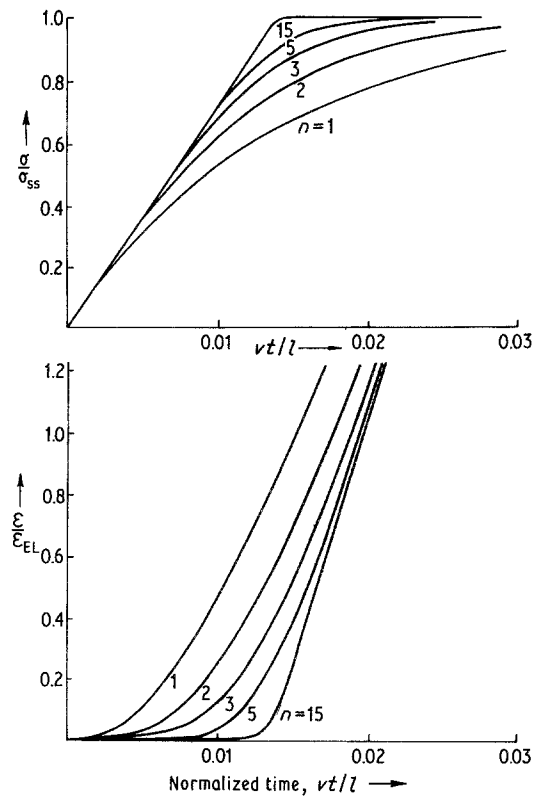


Figure 2 Variation of stress and strain with time for hypothetical materials which have different stress exponent  $n$  and show no strain hardening.

of errors which are likely to arise by the incorrect use of the steady state equation, namely during stress transients.

For power law behaviour ( $\dot{\epsilon} \propto \sigma^n$ ) when  $n > 2$ , no simple analytical solution of Equation 2 is possible and so a finite difference calculation was performed. This involved the calculation of the elastic stress increase after a certain crosshead deflection, then subtracting the stress relaxation due to the creep which occurs in the elapsed time. As the calculation progresses, the new value of the stress is retained for the next step. The results of such a calculation for various  $n$  values are shown in Fig. 2. In the calculation, the values of the creep constants were adjusted to give an identical steady state flow stress. This normalizing procedure allows all the curves to be presented on a single figure. It is to be noted that the transition from predominantly elastic to predominantly plastic behaviour becomes more pronounced with increasing  $n$ .

In Fig. 3 the ratio of the steady state flow stress (“UTS”) and the proof stress is plotted against strain. The ratio is highest for low values of strain

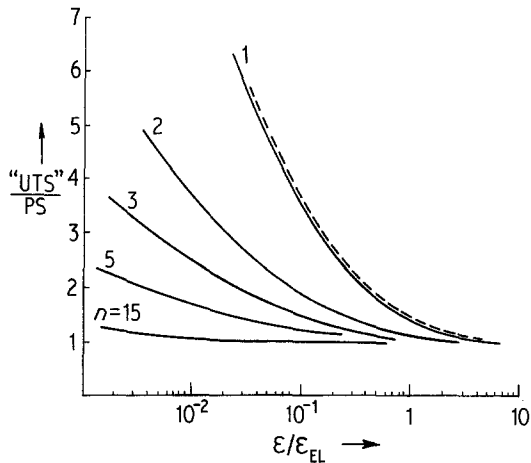


Figure 3 Variation of the ratio of apparent UTS and proof stress with strain for the materials shown in the previous figure. ( $\epsilon_{EL}$  is the elastic strain of the specimen at the steady state flow stress.) The dashed line corresponds to the analytical solution given by Equation 9.

and stress exponent. The ratio approaches unity at large strains. The ratio is independent of the cross-head velocity and creep constant for these cases of constant structure.

### 2.2.3. Threshold stress behaviour

In Fig. 4 the behaviour of stress and strain with time is shown for a creep equation containing a threshold stress,  $\dot{\epsilon} = \alpha_4(\sigma - \sigma_0)^n$ . Values of  $n$  are taken as 1 and 5 in this example. Behaviour is similar to power law creep behaviour in that the elastic-plastic transition is fairly abrupt, even when  $n = 1$ . Once again the "UTS"/PS ratio is close to unity for all but very small strains.

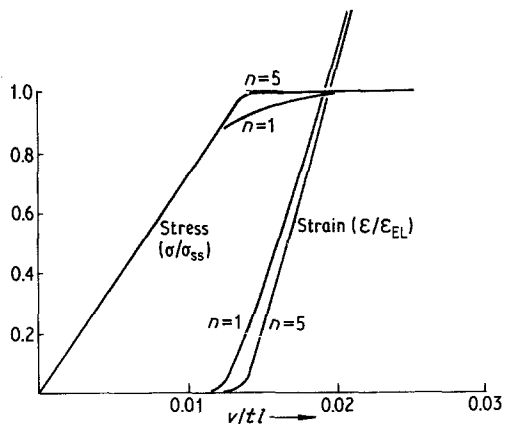


Figure 4 Behaviour of materials which exhibit a flow equation of the form  $\dot{\epsilon} = \alpha(\sigma - \sigma_0)^n$  and which do not work harden.

### 2.3. Influence of recovery processes

As noted in the previous section, thermal recovery processes occur during the testing of materials in the recovery creep regime. New dislocations are being created by the straining process and are annihilated by diffusion controlled recovery. For a three-dimensional dislocation network, the coarsening rate is given by the Friedel [2] equation:

$$\frac{d\lambda}{dt} = \frac{Gb^3 D}{\lambda kT} \quad (12)$$

where  $\lambda$  is the mean network spacing,  $G$  the shear modulus and  $b$  the atomic size. At lower temperatures, dislocation pipe diffusion can contribute to the process and a modification can be incorporated in the above equation to account for this. Thus:

$$\frac{d\lambda}{dt} = \frac{Gb^3 D}{\lambda kT} \left[ 1 + \left( \frac{b}{\lambda} \right)^2 \frac{D_p}{D} \right] \quad (13)$$

$(b/\lambda)^2$  is the ratio of the areas available for the two fluxes, pipe and lattice and  $D_p$  is the dislocation pipe diffusion coefficient.

For plastic flow, the applied stress must exceed  $Gb/\lambda$ , so that in this simple case the flow stress would decay according to:

$$\left( \frac{d\sigma}{dt} \right) = \frac{d\sigma}{d\lambda} \frac{d\lambda}{dt} = - \frac{G^2 b^4 D}{\lambda^3 kT} \left[ 1 + \left( \frac{b}{\lambda} \right)^2 \frac{D_p}{D} \right] \quad (14)$$

However, under the dynamic conditions of a hot tensile test, dislocations are being created each time a slip event occurs. For a simple cubic dislocation network of side length  $x$ , there are twelve dis-

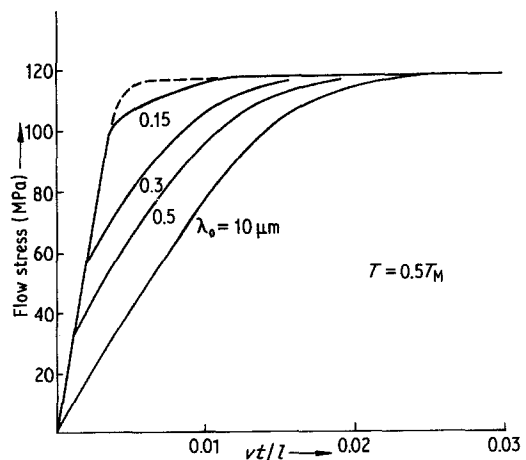


Figure 5 Stress-time plots for materials which show concurrent recovery during test. Curves are shown for a variety of initial dislocation spacings ( $\lambda_0$ ). The dashed line represents the constant structure case from Fig. 3 with  $n = 5$ .

location links of length  $x$ , each shared by four unit cells. This totals  $3x$  of line length per  $x^3$  volume. The dislocation density  $\rho = 3/x^2$ , giving a mean spacing  $\lambda_0 = 1/\rho^{1/2} = x/3^{1/2}$ . A slip event incorporates a further length  $x$  per unit block. The new density is thus  $4/x^2$  and the new spacing  $\lambda = x/2$ . The ratio of spacings before and after a slip event is thus given by  $\sim (3/2)^{1/2}$ .

A computer program was developed which incorporated these unit slip events and coarsening behaviour and matched them to the change in stress in the specimen as the crosshead moves. A given network size is input and the time taken to increase the stress elastically by a given amount is calculated. The amount of coarsening in this time is then calculated from Equation 13. If  $\sigma < Gb/\lambda$  the calculation is performed repeatedly until  $\sigma \geq Gb/\lambda$ . A slip event then gives rise to a strain  $\delta\epsilon = b/\lambda$  which relaxes the stress elastically by an amount  $\delta\sigma = l\delta\epsilon/(K + l/E)$ . A time and strain summation are incorporated in the program, so that  $\sigma$ ,  $\epsilon$ ,  $\lambda$  and  $t$  are known throughout.

Calculations were performed for a typical fcc metal at a homologous temperature  $T = 0.5 T_M$  ( $T_M = 1356$  K) and a crosshead velocity  $V = 5 \times 10^{-7}$  m sec $^{-1}$ , on a specimen of length  $l = 0.05$  m (this gives  $\dot{\epsilon} = 10^{-5}$  sec $^{-1}$  at steady state). An elastic constant  $E = 7 \times 10^4$  MPa was assumed and a machine constant  $K = 1 \mu\text{m MPa}^{-1}$ . Characteristic diffusion coefficients were used as follows:  $D = 5.4 \times 10^{-5} \exp - 18.4 T_M/T \text{ m}^2 \text{ sec}^{-1}$  and  $D_p = 1.88 \times 10^{-5} \exp - 10 T_M/T \text{ m}^2 \text{ sec}^{-1}$ . These values are taken from Brown and Ashby [3]. (The

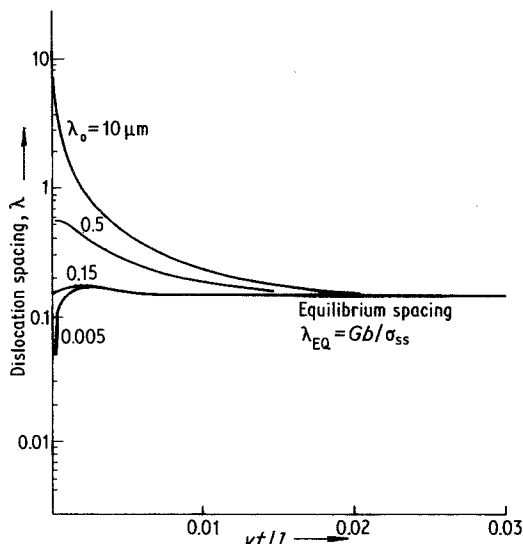


Figure 6 Variation of the dislocation spacing with time for materials having different values of  $\lambda_0$ .

pipe diffusion coefficient is assumed to be identical to the grain-boundary coefficient.) Results are shown in Figs. 5 and 6 for various values of initial dislocation spacing. Constant values of steady state flow stress and dislocation density are achieved, independent of the starting structure. The steady state spacing is defined by  $\lambda = Gb/\sigma_{ss}$ . The flow stress varied as  $\sigma_{ss} \propto (\dot{\epsilon})^{1/5}$ , in agreement with predictions of the dislocation network theory of creep [4] controlled by dislocation pipe diffusion, which gives  $\dot{\epsilon} \propto \sigma^5 D_p$ .

The structural changes which accompany the approach towards the dynamic equilibrium condition are shown graphically in Fig. 6. For an initially coarse structure ( $\lambda_0 = 10 \mu\text{m}$ ), continual refinement occurs towards the equilibrium structure, whereas for a very fine structure ( $\lambda_0 = 0.005 \mu\text{m}$ ), there is sufficient driving force to enable dislocation network growth in the initial stages of the test.

It is the variation in the paths taken towards the steady state condition which is important in determining the proof stress. It should be noted that the strain–time dependence is actually quite similar for all the structures so that the PS is mainly dictated by the instantaneous value of the flow stress in Fig. 5. The ratio “UTS”/PS is plotted in Fig. 7 for two different  $T/T_M$  values. The ratio is seen to vary significantly with temperature, (or, as a corollary, with cross-head speed at constant temperature).

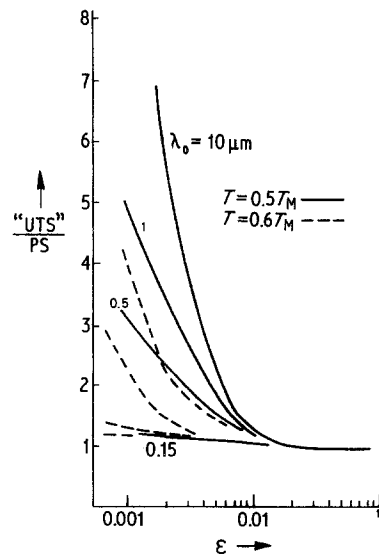


Figure 7 Variation of the ratio “UTS”/PS with strain for materials showing concurrent recovery. The ratio depends on strain, temperature and  $\lambda_0$ .

### 2.3.1. Recovery processes in dispersion hardened systems

When a dispersion of second-phase particles is present, this is likely to influence both plastic slip and thermal recovery. The multiplication process, which involves the formation of dislocation loops between pinning points, may now be dictated by the presence of the second phase as well as the existing dislocation network. If the second-phase particles are widely dispersed, the overall occurrence of slip events will be little different to that in a dispersion-free material. For a finer dispersion, slip can only occur when  $\sigma \geq Gb/\lambda_p$ , where  $\lambda_p$  is the mean inter-particle spacing. Just as there is a particle back stress opposing slip, there is also a similar restriction on network growth. The coarsening rate can probably be represented by an equation of the form of Equation 13 with the driving force for recovery  $Gb^3/\lambda$ , being replaced by  $Gb^3(1/\lambda - 1/\lambda_p)$ , noting that  $d\lambda/dt = 0$  for  $\lambda \geq \lambda_p$ .

Incorporating these modifications into the previous calculation, enables predictions to be made for dispersion hardened systems. A further restriction, on the dislocation density, is imposed by the presence of particles. That is, the initial value of the dislocation spacing probably cannot be greater than the interparticle spacing.

The variation of structure is shown in Fig. 8. In Fig. 8a the interparticle spacing is coarse compared with the steady state spacing ( $\lambda_{EQ}$ ). As a consequence, behaviour is quite similar to particle-free material except for the restriction that  $\lambda_0$  cannot be greater than  $\lambda_p$ . In Fig. 8b, a much finer  $\lambda_p$  is used in the calculation and the equilibrium spacing is only slightly smaller than  $\lambda_p$ . Again

noting the restriction on  $\lambda_0$ , means that spacings  $> \lambda_p$  cannot exist and also, for  $\lambda_0 \ll \lambda_p$ , rapid coarsening occurs in the initial stages so that  $\lambda$  rapidly approaches  $\lambda_p$ . In this case ( $\lambda_p \sim \lambda_{EQ}$ ), the stress-time plot is very similar to that in Fig. 4 with  $n = 5$ .

### 3. Discussion

It is clear from the previous sections that the analysis of the deformation response of materials under the conditions of a hot tensile test at constant displacement velocity is only performed easily for cases where structure remains constant and the stress index is 1 or 2. These cases correspond closely to the deformation mechanisms in crystalline solids of diffusional creep and superplasticity. For both mechanisms, the grain size dictates the diffusive fluxes and boundary sliding rates responsible for strain, so that in principle, the hot tensile test proves a useful technique for study if the grain size remains constant. In practice, diffusional creep rates are often low and this generally precludes the use of the most commonly existing machines. For non-metallics which deform by a Newtonian viscous mechanism, or for superplastic materials which can maintain a fine stable grain size, the technique is ideal, however.

For recovery creep, care has to be taken in the interpretation of results because of the concurrent change in dislocation substructure throughout test. In the analysis given, the recovery is assumed to be the coarsening of the three-dimensional dislocation network according to the Friedel equation and the assumed slip geometry is an approximation to the real processes operating. No account is taken of the role of localized sub-grain walls which are

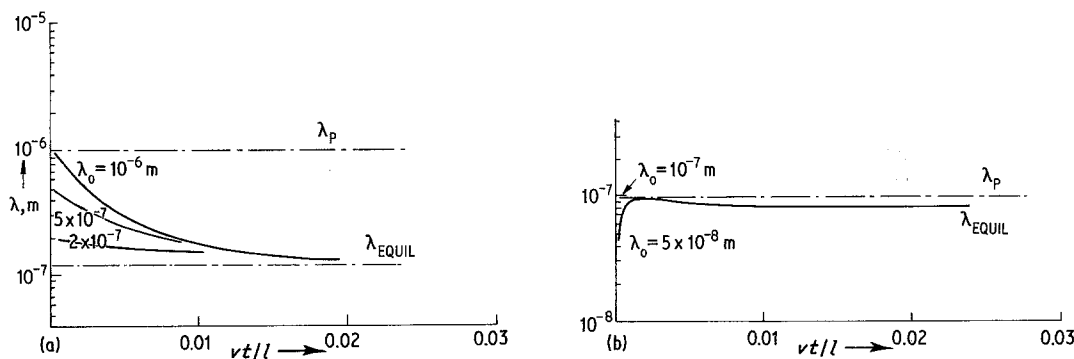


Figure 8 Variation of dislocation spacing in dispersion-hardened materials. In (a) the particle spacing is much greater than the equilibrium spacing so that behaviour is similar to the particle-free material apart from the limitation that  $\lambda_0 \leq \lambda_p$ . In (b)  $\lambda_p$  is much closer to  $\lambda_{EQ}$  so that little change in structure is allowed. The stress-time behaviour closely resembles the structure-insensitive behaviour of Fig. 4.

known to form in addition to the more general three-dimensional network and the examples are limited to the case where the slip event may be considered rapid in comparison with recovery. This is not always the case. Dislocation glide may, for example, be limited by the dragging force of a solute atmosphere, in which case the glide events will occur at a much slower rate.

A further feature which is omitted from the calculations is the change in stress which occurs as a result of loss of specimen cross-section by the straining process. Such features are important when specimens are extended to large strains, but for the purposes of the present calculations, where the structural transients leading to the steady state are complete in less than 1% strain, then large strain features are unimportant.

Given these limits set upon the calculations, several conclusions may be made with some confidence.

#### 4. Conclusions

For a material which undergoes creep by a mechanism which involves no structural changes, the rate of stress increase during a tensile test is solely dictated by the elastic deflection of the system and the concurrent stress relaxation by creep.

Newtonian viscous solids represent such a class of materials and exhibit an inverse exponential stress increase with time. The initial slope corresponds to the elastic constants and the limiting value to the steady state flow stress. The proof stress, defined as the flow stress at some reference strain, is related directly to the creep constant. The ratio of the proof stress to the steady state flow stress ("UTS") is independent of the ratio: creep constant/crosshead speed.

Superplastic materials represent another class of materials which undergo no significant structural changes during flow. For these materials the flow

stress increases with  $\tanh t$ . The PS/"UTS" ratio is again independent of testing conditions.

In order to predict behaviour for materials which deform by recovery creep, it is necessary to make assumptions about the mechanisms responsible for plastic slip and recovery. Accurate calculations made using simple models of these processes, enable general conclusions to be made for real materials.

If the initial dislocation density is low, then the "UTS"/PS ratio is high and the form of the  $\sigma-t$  curve is much different to the constant structure case. The ratio also becomes dependent of cross-head speed and temperature. At higher initial densities, the curve approaches more closely that for constant structure.

If a dispersion of second-phase particles exists, a limit is set upon the initial density. If the dispersion is widely spaced, compared to  $Gb/\sigma_{ss}$ , the behaviour is little different to particle-free material. For fine dispersions, however, the limitation imposed by the particle spacing on the initial dislocation density can mean that little structural change may be required during test so that the  $\sigma-t$  plot corresponds closely to the constant structure case.

#### Acknowledgement

This paper is published by permission of the Central Electricity Generating Board.

#### References

1. B. BURTON, "Diffusional Creep of Polycrystalline Materials" (Trans. Tech. SA, Switzerland, 1977).
2. J. FRIEDEL, "Dislocations" (Pergamon, Oxford, 1964).
3. A. M. BROWN and M. F. ASHBY, *Acta Metall.* **28** (1980) 1085.
4. B. BURTON, *Phil. Mag.* **45A** (1982) 657.

*Received 8 August  
and accepted 13 September 1983*